International Journal of Pharmaceutics 365 (2009) 206–213

Contents lists available at ScienceDirect

International Journal of Pharmaceutics

journal homepage: www.elsevier.com/locate/ijpharm

Pharmaceutical Nanotechnology

Entrapment and release of saquinavir using novel cationic solid lipid nanoparticles

Yung-Chih Kuo*, Hung-Hao Chen

Department of Chemical Engineering, National Chung Cheng University, Chia-Yi 62102, Taiwan, ROC

ARTICLE INFO

Article history:
Received 15 April 2008
Received in revised form 3 July 2008
Accepted 25 August 2008
Available online 19 September 2008

Keywords:
Cationic solid lipid nanoparticle
Saquinavir
Entrapment
Release

ABSTRACT

Cationic solid lipid nanoparticles (CSLNs) with entrapped saquinavir (SQV) were fabricated by microemulsion method. Here, CSLNs were stabilized by polysorbate 80, and the lipid phase contained cationic stearylamine (SA) and dioctadecyldimethyl ammonium bromide (DODAB) and nonionic Compritol 888 ATO (CA) and cacao butter (CB). Properties of the present pharmaceutical formulations including the entrapment efficiency, the release kinetics, and the distribution of SQV in CSLNs were analyzed. The results indicated that a mixture of SA and DODAB and a mixture of CA and CB were beneficial to the entrapment efficiency of SQV. However, an increase in the content of cationic lipids insignificantly affected the entrapment efficiency of SQV when the weight percentage of SA and DODAB was greater than 1% during emulsification. Also, the rate of SQV released from CSLNs with lipid cores of a mixture of CA and CB was slower than that of pure CB. The temporal variation in the released SQV suggested that the carriers could be sustained delivery systems with no apparent initial burst. Hence, the current CSLNs could carry SQV for the improved medication of individuals infected by human immunodeficiency viruses.

1. Introduction

Saquinavir (SQV) is a protease inhibitor used in the clinical treatment for the acquired immunodeficiency syndrome (AIDS), which is derived from the infection of human immunodeficiency virus (HIV). During the infectious stage, the cleavage position of precursor proteins in HIV can only be recognized by specific viral proteases. Thus, SQV is designed as a peptide similar to the cleavage position for association with the proteases in HIV-1 and HIV-2. Note that $\log D_{oct}$ (the logarithm of the octanol/buffer partition coefficient) of SQV at pH 7.4 is 4.51, indicating that SQV is a rather lipophilic anti-HIV agent. In physiology, the fundamental properties of SQV are 1 h of resident period in blood, 98% of binding to plasma proteins, and 13.2 h of elimination half life for tissue linkage (Lemberg et al., 2002; Strazielle et al., 2005). The main defect of SQV is the low bioavailability of 4–12% (Williams and Sinko, 1999). Besides, SQV belongs to the P-glycoprotein (P-gp) substrate, which is liable to be modulated by the mediation mechanism of P-gp (Lee, 2000; Polli et al., 1999). For transport across the blood–brain barrier, SQV is also inhibited by P-gp (Bachmeier et al., 2005). To improve the absorption rate, dipeptide prodrugs of SQV were designed and demonstrated for shunning the efflux by P-gp (Jain et al., 2007). Except the modification with prodrugs, another efficacious method for enhancement in the bioavailability of SQV is the carrier-mediated system.

The traditional carriers for anti-HIV agents included emulsions, liposomes, polymeric microparticles, and nanoparticles (Kuo and Chung, 2005). For brain-targeting delivery, solid lipid nanoparticles (SLNs) exhibited the typical advantages of nanoparticulate carriers with excellent biocompatibility (Kuo and Kuo, 2008). Moreover, SLNs could extend the half-life of pharmaceuticals in blood and the scale-up feasibility of SLNs was high in practical manufacturing (Bargoni et al., 1998). SLNs were also capable of entrapping antitumor FUdR and carrying FUdR into the central nervous system (Wang et al., 2002). By pharmacokinetic analysis, SLNs were concluded to be a qualified colloidal transporter for the delivery of camptothecin into the brain, the heart, and the reticuloendothelial system (Yang et al., 1999). Furthermore, positively charged carriers were beneficial to the loading of drugs (Kuo, 2005) and to the cellular uptake via electrostatic interactions (Kuo and Lin, 2006). In a study on the binding capacity and the transfection efficiency of genes, cationic SLNs (CSLNs) containing nonionic lipids of Compritol ATO 888 (CA) and cetylpalmitate were prepared (Tabbatt et al., 2004). It was concluded that one-tailed cationic lipids were more toxic than two-tailed cationic lipids such as dioctadecyldimethyl ammonium bromide (DODAB). For CSLNs composed of one-tailed stearylamine (SA), stable complexes of CSLNs, DNA, and

Abbreviations: CA, Compritol 888 ATO; CB, cacao butter; CSLNs, cationic solid lipid nanoparticles; DODAB, dioctadecyldimethyl ammonium bromide; SA, stearylamine; SQV, saquinavir.

* Corresponding author. Tel.: +886 5 272 0411x33459; fax: +886 5 272 1206.
E-mail address: chmyck@ccu.edu.tw (Y.-C. Kuo).

0378-5173/$ – see front matter © 2008 Elsevier B.V. All rights reserved.
doi:10.1016/j.ijpharm.2008.08.050

Nomenclature

D	Z-average diameter of CSLNs (nm)
E_e	entrapment efficiency of SQV in CSLNs (%)
$P_{(CA+CB+SQV)/EM}$	weight percentage of nonionic lipids and SQV during emulsification (%)
$P_{CB/(CA+CB)}$	weight percentage of CB in nonionic lipids (%)
$P_{DODAB/EM}$	weight percentage of DODAB during emulsification (%)
$P_{(DODAB+SA)/EM}$	weight percentage of cationic lipids during emulsification (%)
$P_{SA/(DODAB+SA)}$	weight percentage of SA in cationic lipids (%)
$P_{SA/EM}$	weight percentage of SA during emulsification (%)
P_{SQV}	percentage of SQV released from CSLNs (%)
$P_{SQV/(CA+CB+SQV)}$	weight percentage of SQV in nonionic lipids and SQV (%)

Greek letter

ζ	zeta potential of CSLNs (mV)

streptavidin with the binding of biotinylated ligands yielded a high affinity to cellular receptors (Pedersen et al., 2006). Also, the bioavailability and the distribution of anti-psychotic clozapine in the brain were enhanced by the entrapment in CSLNs with cationic SA (Manjunath and Venkateswarlu, 2005). These results implied that CSLNs can be appropriate for carrying lipophilic SQV with ameliorated delivery behavior. For the entrapment of SQV, the internal lipids with complicated biocompatible components were generally required (Müller et al., 2000). Hence, a mixture of CA and cacao butter (CB) (Kim et al., 2005) was employed as the nonionic ingredients of lipid cores in the current CSLNs.

In this study, SQV-entrapping CSLNs with a mixture of CA and CB in the central lipid phase and a mixture of SA and DODAB in the peripheral lipid phase were prepared. Polysorbate 80 in the external layer of CSLNs could prevent the particles from coagulation. The following parameters for the entrapment efficiency of SQV in CSLNs were examined: the ratio of CA to CB, the ratio of SA to DODAB, the content of cationic lipids, and the amount of SQV. Since CA and CB provided various entrapping sites for lipophilic drugs, the distribution of SQV in CSLNs was studied by the nuclear magnetic resonance (NMR). Furthermore, the in vitro dissolution for the release of entrapped SQV from CSLNs was especially analyzed.

2. Materials and methods

2.1. Reagents and chemicals

Dulbecco's phosphate-buffered saline (DPBS), D-mannitol, DODAB, sodium azide, and glutaraldehyde were purchased from Sigma (St. Louis, MO). Deuterium oxide-D was obtained from Cambridge Isotope Laboratories, Inc. (Andover, MA), SQV from United States Pharmacopeial (Rockville, MD), polysorbate 80 from FisherScientific (Fair Lawn, NJ), cacao butter (CB) from OCG Cacao (Whitinsville, MA), CA from Gattefosse S. A. (at Parc des Barbanniers, 92632 Gennevilliers, France), SA from Fluka (Buchs, Switzerland), ethanol from Riedel-de Haën (Seelze, Germany), acetonitrile from BDH (Poole, England), and ultrapure water from Nanopure Infinity Ultrapure System of Barnstead (Dubuque, IA).

2.2. Preparation of SQV-entrapping CSLNs

SQV-entrapping CSLNs with nonionic lipids of CA and CB and cationic lipids of SA and DODAB were fabricated by microemulsion method described previously (Kuo and Su, 2007) with modifications. Briefly, based on the overall microemulsified fluid, 4% (w/w) nonionic lipids and SQV was mixed with cationic lipids under magnetic stirring at 75 °C. 8% (w/w) polysorbate 80 and 7.5% (w/w) ethanol were dissolved in ultrapure water and preheated at 75 °C. The compositions of the primary microemulsions are summarized in Table 1. The surfactant solution was mixed with the melted lipids and SQV at 500 rpm and 75 °C for 3 min. One aliquot of the microemulsified liquid was added into 10 aliquots of ultrapure water at 500 rpm and 3 °C for 20 min. The suspension containing newly formed CSLNs was filtrated by a filtration paper with pores of 1 μm. SQV-entrapping CSLNs in the filtrate were separated by a refrigerated superspeed centrifuge (CP80MX, Hitachi Koki, Tokyo, Japan) with a rotor of P40ST-1591 in a conical centrifugal microtube (Falcon, Franklin Lakes, NJ) at 236,500 × g for 30 min. Bottom pellet containing CSLNs of 60 mg was resuspended in ultrapure water of 10 mL with 2% (w/v) D-mannitol, refrigerated at 4 °C for 30 min, at −20 °C in a low temperature freezer (Frigidaire, Augusta, GA) for 30 min, and at −80 °C in an ultralow temperature freezer (Sanyo, Osaka, Japan) for 30 min, and lyophilized at −80 °C and 4 Pa (Eyela, Tokyo, Japan) over 24 h to obtain powder products. The existence of CSLNs in the supernatant was checked by a zetasizer 3000 HS_A (Malvern, Worcestershire, UK) for confirmation of the completion in centrifugal separation. The supernatant was also applied to the estimation of the entrapment efficiency.

Several formulations of CSLNs were obtained by alteration in the ratio of CA to CB, the weight percentage of SA and DODAB, the ratio of SA to DODAB, and the weight percentage of SQV. For the high resolution proton nuclear magnetic resonance (^{1}H NMR) analysis, CSLNs were prepared without ethanol and D-mannitol.

2.3. Entrapment efficiency of SQV

The wavelength of UV absorbance for SQV was scanned by a UV microplate spectrophotometer (Bio-Tek, Winooski, VT) in the range of 200–400 nm and the maximal absorbance was 239 nm, which was consistent with the literature result (Glynn and Yazdanian, 1998). The amount of SQV in the supernatant after centrifugation was evaluated by a high performance liquid chromatography (Jasco, Tokyo, Japan) with a UV–vis spectrophotometer (UV-2075 Plus, Jasco, Tokyo, Japan) at 239 nm. A reverse phase BDS Hypersil C18 column containing particles of 5 μm (Thermo Hypersil-Keystone, Bellefonte, PA) was warmed by a column heater (Alltech, Derrfield, IL) at 45 °C. Two high-pressure pumps (PU-2080 Plus, Jasco, Tokyo, Japan) in series were applied to the mobile phase containing ultrapure water and acetonitrile with the gradient from 20 to 50% in 20 min with a fluid flow rate of 0.85 mL/min. The retention time of SQV was about 8.7 min and the R-squared value for the calibration of SQV at 239 nm was about 0.99. The entrapment efficiency, E_e, was calculated by:

$$E_e = \frac{\text{total weight of SQV} - \text{weight of SQV in supernatant}}{\text{total weight of SQV}} \times 100\%$$

2.4. Characterization of SQV-entrapping CSLNs

2.4.1. Particle size and morphology

The particle size distribution, the cumulant Z-average diameter, and the zeta potential of SQV-entrapping CSLNs were obtained by a zetasizer 3000 HS_A with a photon correlation spectroscope and a Laser Doppler velocimeter (Malvern, Worcestershire, UK) at 25 °C. CSLNs in ultrapure water with a concentration of 2 mg/mL were employed in the detection. The duration of the detection was 120 s for the particle size distribution and the average diameter and was 20 s for the zeta potential. The assumptions for the calcu-

Table 1
Weight percentage (%) of primary microemulsions in the fabrication of SQV-entrapped CSLNs.

	SQV	CA	CB	SA	DODAB	Water
Variation in $P_{CB/(CA+CB)}$ and $P_{SA/EM}$	0.2	3.8	0	0	0	80
		1.9	1.9	0.5		
		0	3.8			
		3.8	0	1		79.5
		1.9	1.9			
		0	3.8			
		3.8	0	1.5		79
		1.9	1.9			
		0	3.8			
		3.8	0	2		78.5
		1.9	1.9			
		0	3.8			
Variation in $P_{CB/(CA+CB)}$ and $P_{DODAB/EM}$		3.8	0	0	0.5	80
		1.9	1.9			
		0	3.8			
		3.8	0		1	79.5
		1.9	1.9			
		0	3.8			
		3.8	0		1.5	79
		1.9	1.9			
		0	3.8			
		3.8	0		2	78.5
		1.9	1.9			
		0	3.8			
Variation in $P_{SQV/(CA+CB+SQV)}$ and $P_{SA/(DODAB+SA)}$	0.1	1.95	1.95	0	1	79.5
				0.33	0.67	
				0.5	0.5	
				0.67	0.33	
				1	0	
	0.2	1.9	1.9	0	1	
				0.33	0.67	
				0.5	0.5	
				0.67	0.33	
				1	0	
	0.3	1.85	1.85	0	1	
				0.33	0.67	
				0.5	0.5	
				0.67	0.33	
				1	0	
Variation in $P_{CB/(CA+CB)}$		0	3.7	0.5	0.5	
		1.85	1.85			

Ethanol and polysorbate 80 were, respectively, 7.5 and 8% in every preparation.

lation of the particle size distribution included sphericity of CSLNs without multiple scattering. To avoid the interference by bubbles, resuspended CSLNs were injected gradually into a quartz tube. The surface microstructure of CSLNs was analyzed by a field emission scanning electron microscope (FE-SEM, JSM-6330 TF, JOEL, Tokyo, Japan). The samples were mounted on a specimen stub by conductive carbon paint, and then vacuum-dried and sputter-coated with platinum. Note that the carbon paint was used for the attachment of CSLNs. The sputter coating caused the deposition of platinum for only several layers. Thus, these treatments would not lead to alterations in the apparent structure of the particle surfaces.

2.4.2. Nuclear magnetic resonance

The spectra of ^{1}H NMR for CSLNs with lipid cores of a mixture of CA and CB, CSLNs with lipid cores of pure CB, the reference system of polysorbate 80, and the reference system of SQV were obtained by a DPX-400 spectrometer (Bruker, Rheinstätten, Germany) at 400 MHz and 37 °C. The primary microemulsions included internal lipids of 3.7% (w/w) CB or 1.85% (w/w) CB and 1.85% (w/w) CA, 0.3% (w/w) SQV, 0.5% (w/w) SA, 0.5% (w/w) DODAB, 8% (w/w) polysorbate 80, and 87% (w/w) ultrapure water. SQV-entrapping CSLNs of 0.3 mg were mixed with D_2O of 1 mL to form 0.03% (w/v) suspension for the ^{1}H NMR study. In a study on the entrapment capacity, the distribution of lecithin in SLNs was analyzed by NMR with the reference systems of pure lecithin and pure surfactant (Schubert et al., 2006). Thus, polysorbate 80 and SQV in D_2O were selected as the reference systems. The reference systems of surfactant and drug were, respectively, 0.0185% (w/v) polysorbate 80 and 0.0004% (w/v) SQV in D_2O. An aliquot of the sample was placed in an NMR tube (Schott, Mainz, Germany) with the addition of deuterium oxide-D from the glass capillaries for field login. The specimens were ultrasonically vibrated with the on-off alternative rhythm of every 30 s for 30 min before detection.

2.4.3. Release of SQV from CSLNs

0.5% (w/v) SQV-entrapping CSLNs was resuspended in DPBS containing 0.05% sodium azide. The suspension was placed in a baths-reciprocal shaker at 60 rpm and 37 °C over 48 h. At specific time interval, the samples with released SQV were centrifuged at 236,500 × *g* and 25 °C for 30 min. Procedures for the assessment of the amount of SQV in the supernatant were the same as those described in Section 2.3.

3. Results and discussion

3.1. Size and morphology of SQV-entrapping CSLNs

The typical distribution of the particle diameter in intensity and the SEM micrographs of SQV-entrapping CSLNs are displayed in Fig. 1. As revealed in Fig. 1(a), the particle diameter in this batch

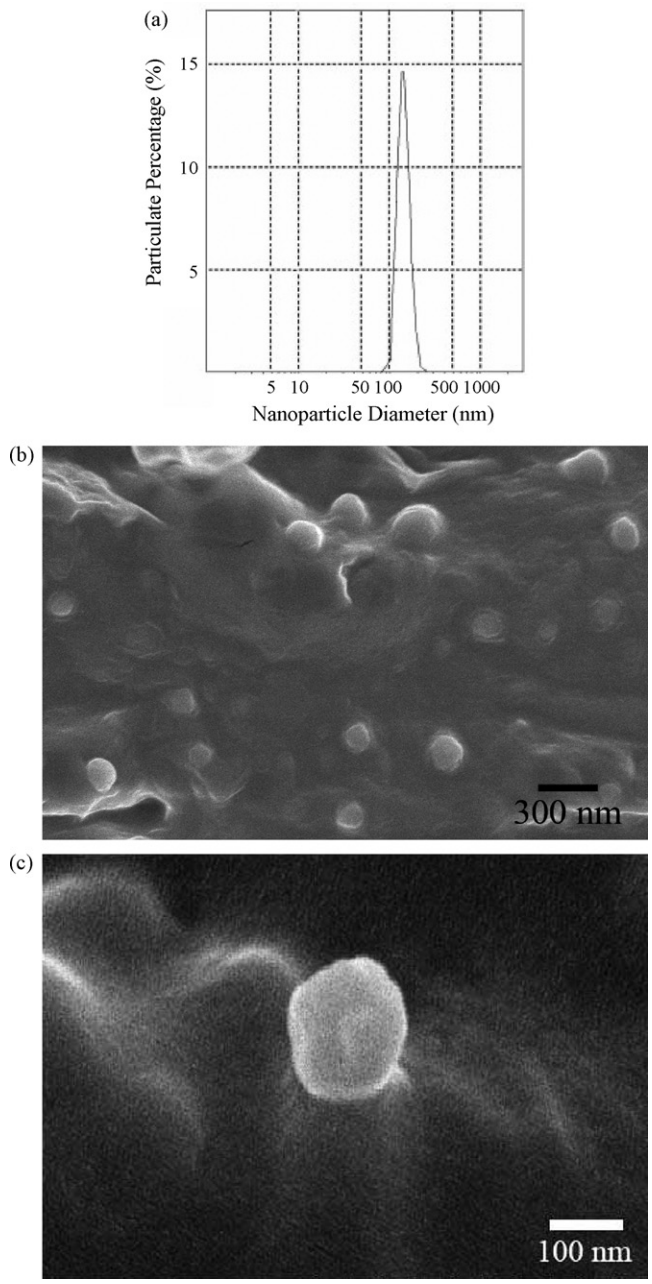

Fig. 1. Typical diameter distribution and SEM images of SQV-entrapped CSLNs. $P_{CB/(CA+CB)}$ = 50%, $P_{SA/(DODAB+SA)}$ = 50%, $P_{SQV/(CA+CB+SQV)}$ = 7.5%, $P_{(CA+CB+SQV)/EM}$ = 4%, and $P_{(DODAB+SA)/EM}$ = 1%: (a) particle diameter distribution, (b) FE-SEM image, and (c) close-up FE-SEM image.

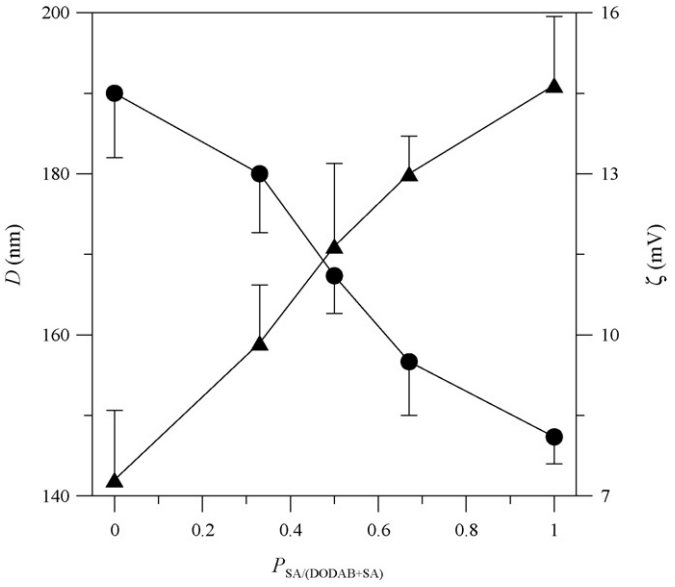

Fig. 2. Average diameter and zeta potential of CSLNs. $P_{CB/(CA+CB)}$ = 50%, $P_{SQV/(CA+CB+SQV)}$ = 7.5%, $P_{(CA+CB+SQV)/EM}$ = 4%, and $P_{(DODAB+SA)/EM}$ = 1%: (▲) for average diameter and (●) for zeta potential. n = 3.

was narrowly distributed. In the present study, various colloidal products were synthesized by alterations in the composition of nonionic lipids, the composition of cationic lipids, and the amount of incorporated SQV. As exhibited in Fig. 1(b), the ellipsoidal particles were prepared. This image was consistent with the result of Fig. 1(a). As presented in Fig. 1(c), some superficial lumps and pits were observed, indicating a slightly rough surface. Fig. 2 shows the variation in the average diameter and the zeta potential of SQV-entrapping CSLNs as a function of the composition of cationic lipids. The average diameter and the zeta potential of SQV-entrapping CSLNs ranged roughly between 140 and 190 nm and between 8 and 14.5 mV, respectively. As displayed in Fig. 2, an increase in the level of SA led to an increase in the average diameter and a decrease in the zeta potential. This was mainly because the dissociation of bromine from DODAB was easier than the absorption of proton by SA during emulsification. Hence, an increase in the level of SA caused a decrease in the positive charge on the polysorbate 80-coated CSLNs. In a study on the electrokinetic behavior of CSLNs with internal cores of CB, an increase in the particle diameter resulted also from an increase in the level of SA (Kuo and Lin, 2008). The range of polydispersity indices was between 0.02 and 0.37, and the quite broad range of polydispersity indices pointed normally to the differences among formulations. For the batches with small polydispersity indices, the relatively monodispersed suspensions might result also from a constant stirring rate, a constant temperature, and a constant period for the formation of CSLNs during the fabrication processes.

3.2. Effect of cationic lipids and SQV on the entrapment efficiency

Fig. 3 shows the effect of the level of SA on the entrapment efficiency of SQV. Here, SA was the only cationic lipid in CSLNs. As indicated in this figure, the entrapment efficiency for $P_{SA/EM}$ = 1% was larger than that for $P_{SA/EM}$ = 0.5%. However, the entrapment efficiency was almost not affected by an increase in $P_{SA/EM}$ when $P_{SA/EM} \geq 1\%$. This suggested that a nearly constant entrapment efficiency was achieved when the ratio of $P_{SA/EM}$ to $P_{(CA+CB+SQV)/EM}$ was greater than 0.25 (1:4). For a constant $P_{SA/EM}$, the order of the entrapment efficiency followed $P_{CB/(CA+CB)}$ = 50% > $P_{CB/(CA+CB)}$ = 0% > $P_{CB/(CA+CB)}$ = 100%. This indicated that the lipid cores composed of a mixture of CA and CB provided more vacancies for SQV than those of pure lipid (CA or CB). Also, CA was more efficacious in the entrapment of SQV than CB. Note that the composition of CA reported by the supplier (Gattefosse S. A.) is 28–32% tribehenate, 52–54% dibehenate, and 12–18% monobehenate. Also, CB comprises of four triglycerides of 24.4–26.2% palmitic acid (C16), 34.4–35.4% stearic acid (C18), 37.7–38.1% oleic acid (C18:1), and 2.1% linolenic acid (C18:3) (Liendo et al., 1997). Lipids with similar molecular configurations might produce crystalline structure with a few spaces for the incorporation of SQV. Hence, a highly ordered lattice could not imbed a large amount of SQV, which was usually accommodated between lipid

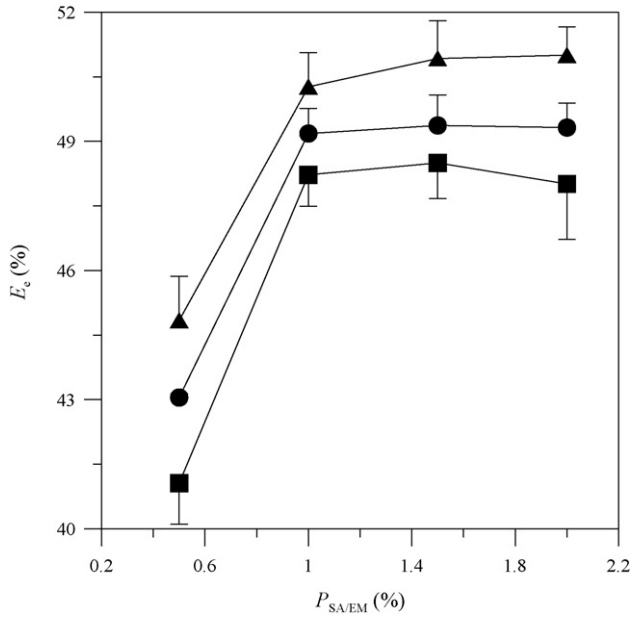

Fig. 3. Entrapment efficiency of SQV in CSLNs for $P_{SA/(DODAB+SA)}$ = 100%, $P_{SQV/(CA+CB+SQV)}$ = 5% and $P_{(CA+CB+SQV)/EM}$ = 4%: (▲) for $P_{CB/(CA+CB)}$ = 50%, (●) for $P_{CB/(CA+CB)}$ = 0%, and (■) for $P_{CB/(CA+CB)}$ = 100%. n = 3.

layers and among molecular chains. Moreover, the complex structure of lipid cores with molecules of tri-, di-, and mono-behenate and with various chain lengths was beneficial to the entrapment of SQV. The effect of the level of DODAB on the entrapment efficiency of SQV is presented in Fig. 4. Here, DODAB was the only cationic lipid in CSLNs. Results shown in Fig. 4 were analogous to those in Fig. 3. Note that polysorbate 80 might form micells beside lipids in the present microemulsions. Also, the micellar structure in pharmaceutical formulations was able to solubilize drug (Momot et al., 2003). Nevertheless, SQV was first mixed in lipids in the present preparation and could be tightly captured by the lipid matrix because of its high lipophilicity. Hence, limited SQV could diffuse into the surfactant phase during the short period of emulsification (3 min) although the concentration of polysorbate 80 was higher than that of lipids. During centrifugation, CSLNs and detached polysorbate 80 might be condensed at the bottom of the centrifugal microtube. However, SQV in the solidified CSLNs could hardly migrate into the polysorbate 80-rich fluid region. In a study on the loading and sustained release of drug, lipid nanoparticles were fabricated by one of the following saturated crystalline triglycerides: trimyristin, Witepsol H 35, H 42, and E 85 (Westesen et al., 1997). As compared with the lipid nanoparticles of Westesen et al., the internal lipid cores of a mixture of CA and CB in the present CSLNs were much more complicated and were unlikely to form the stable β-form. As a result, the present formulations yielded smaller crystal zones, slower phase-transition rate, and weaker drug-expulsion ability. Besides, abrupt cooling to 3 °C might prevent the lipid components from crystallization. Owing to the complication of the lipid matrix, no precipitate was observed even after resuspension of the lyophilized powders. Moreover, no long-term storage was applied to the present CSLNs. Thus, phase transition of the lipid matrix produced negligible influence on the distribution of SQV in CSLNs.

Fig. 5 shows the effect of the weight percentage of SA in the cationic lipids of CSLNs on the entrapment efficiency of SQV. Here, the weight ratio of CA to CB was 1 and the weight ratio of cationic lipids to nonionic lipids and SQV was 0.25. As indicated in Fig. 5, the maxima of the entrapment efficiency occurred when the weight ratio of SA to DODAB was 1 ($P_{SA/(DODAB+SA)}$ = 0.5). Note that the carbohydrate portion in the structure of SA and DODAB exhibited single-tail and double-tails, respectively. For the two cationic lipids, charged head group normally pointed outwards in the peripheral zones of lipid cores. On the other hand, the hydrophobic chains of SA and DODAB provided more intermingled spaces for the incorporation of SQV. As revealed in Fig. 5, an increase in the amount of SQV yielded a decrease in the entrapment efficiency. This was because the solubility of SQV in the melted lipids and the overall content of lipids were constant. Thus, for a high amount of SQV, competition

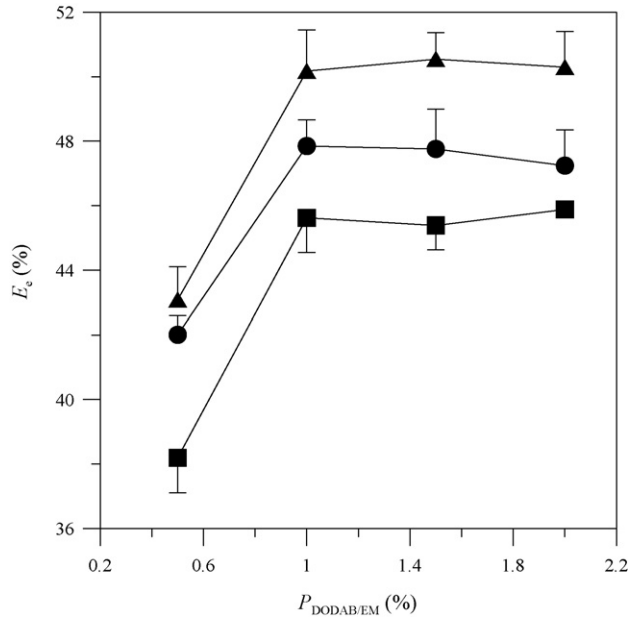

Fig. 4. Entrapment efficiency of SQV in CSLNs for $P_{SA/(DODAB+SA)}$ = 0%, $P_{SQV/(CA+CB+SQV)}$ = 5% and $P_{(CA+CB+SQV)/EM}$ = 4%: (▲) for $P_{CB/(CA+CB)}$ = 50%, (●) for $P_{CB/(CA+CB)}$ = 0%, and (■) for $P_{CB/(CA+CB)}$ = 100%. n = 3.

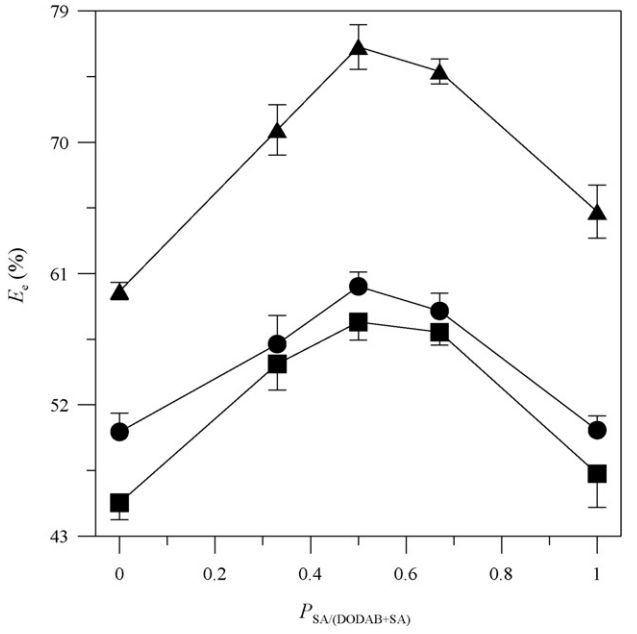

Fig. 5. Variation in entrapment efficiency of SQV in CSLNs as a function of weight percentage of SA in cationic lipids. $P_{CB/(CA+CB)}$ = 50%, $P_{(CA+CB+SQV)/EM}$ = 4%, and $P_{(DODAB+SA)/EM}$ = 1%: (▲) for $P_{SQV/(CA+CB+SQV)}$ = 2.5%, (●) for $P_{SQV/(CA+CB+SQV)}$ = 5%, and (■) for $P_{SQV/(CA+CB+SQV)}$ = 7.5%. n = 3.

of SQV for the fixed content of entrapping sites in the lipid phase led to low entrapment efficiency. Note that the results of the present CSLNs were consistent with the results of the negatively charged SLNs (Kuo and Su, 2007).

3.3. Analysis of ^1H NMR spectra

Fig. 6(a) exhibits the ^1H NMR spectra of CSLNs and the reference systems. The functional groups of the reference systems were symbolized in Fig. 6(b). For polysorbate 80, the proton symbols for the corresponding chemical shift, δ_H, were: (a) 0.8 ppm, (b) 1.2 ppm, (c) 1.5 ppm, (d) 1.9 ppm, (e) 2.25 ppm, (f) 3.6 ppm, (g) 4.1 ppm, and (h) 5.1–5.3 ppm (Cross, 1987; Momot et al., 2003). For SQV, the benzene rings in the drug molecule were unique in the present CSLNs. The proton symbols for the corresponding δ_H were: (α) 6.7 ppm, (β) 6.9 ppm, (γ) 7.1 ppm, (δ) 7.75 ppm, (ε) 7.9 ppm, (ζ) 8.05 ppm, (η) 8.1 ppm, (θ) 8.14 ppm, and (ι) 8.5 ppm (Boudad et al., 2001). δ_H at 4.7 ppm represented the signal of H_2O. Also, the *Z*-average diameters of CSLNs were: 184.7 nm for the sample of spectrum (II) and 221.1 nm for the sample of spectrum (III). As compared with Fig. 2, the increases in the average diameters resulted mainly from the nonuse of ethanol (cosurfactant) and mannitol (cryoprotectant). Although ethanol could inhibit augmentation in the drop diameter, sufficient fluidic shear stress during emulsification might restrain the droplets from growth (Kuo and Chen, 2007). Abandonment of mannitol however yielded appreciable aggregation of CSLNs.

As compared with spectrum (I), the signals of a–h in spectra (II) and (III) decreased significantly, implying the interaction

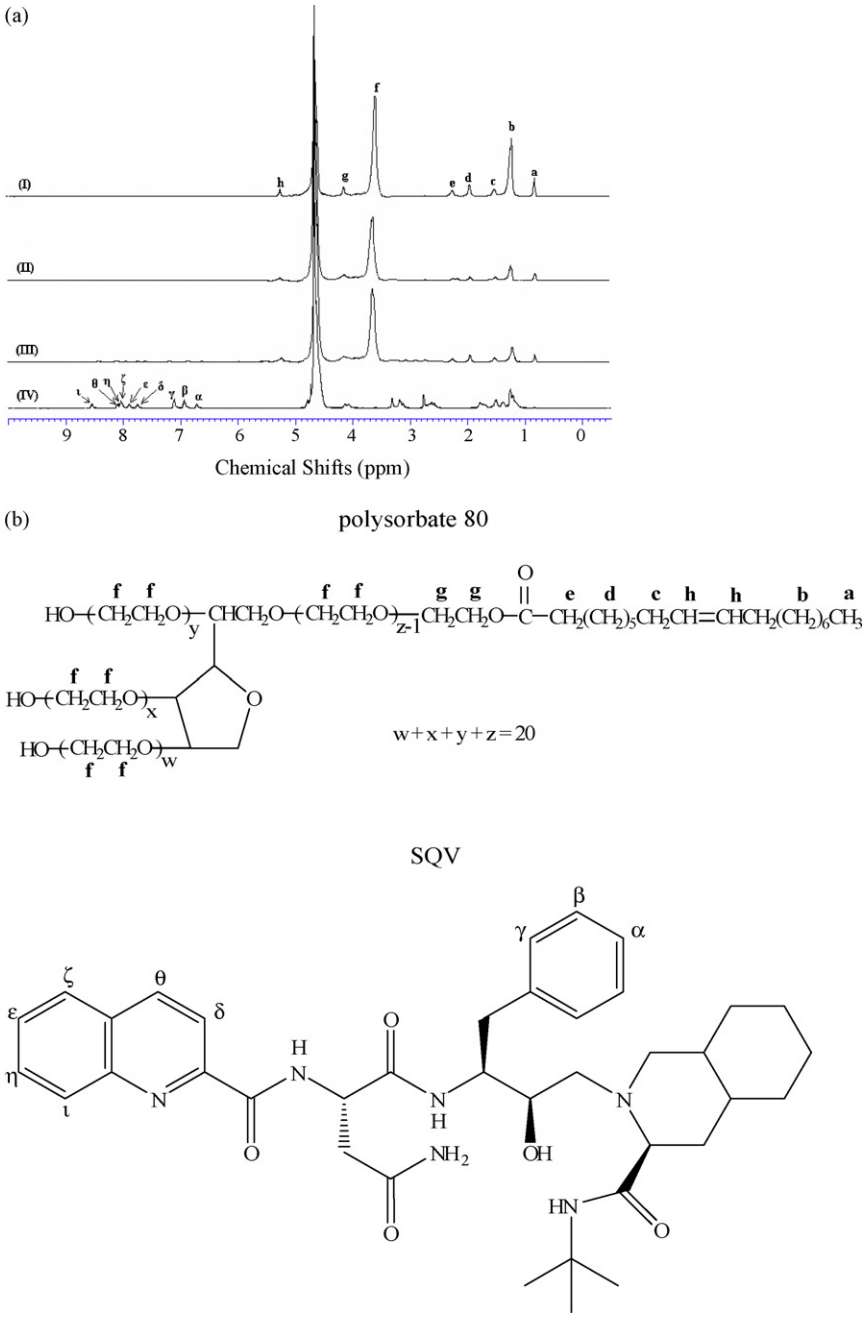

Fig. 6. ^1H NMR spectra of the following systems: (I) polysorbate 80 in D_2O, (II) SQV-entrapped CSLNs with $P_{CB/(CA+CB)}$ = 50% in D_2O, (III) SQV-entrapped CSLNs with $P_{CB/(CA+CB)}$ = 100% in D_2O, and (IV) SQV in D_2O. (II) and (III) $P_{SA/(DODAB+SA)}$ = 50%, $P_{SQV/(CA+CB+SQV)}$ = 7.5%, $P_{(CA+CB+SQV)/EM}$ = 4%, and $P_{(DODAB+SA)/EM}$ = 1%.

between the carbon chain of polysorbate 80 and the lipid phase. The apparent decrease in magnitude of the signals of a and b suggested that strong bindings hindered mobility of the hydrophobic tails of polysorbate 80. The magnitude of decrease in the signal of f was relatively unobvious. This indicated that mobility of the outward hydrophilic head groups maintained comparably high with the preference of the groups for water phase. As compared with spectrum (IV), no chemical shift corresponding to the signals of α–ι in spectra (II) were observed. Very weak signals of α–ι in spectra (III) were detected. Spectrum (II) suggested that protons of the benzene ring in SQV were embedded inside lipid cores of CSLNs and were sterically obstructed by CA and CB, leading to no resonant response by the magnetic influence. This result also inferred that SQV might be concentrated in the interior cores of a mixture of CA and CB or uniformly distributed over the lipid phase. Also, a large discrepancy in molecular weights of the components in CA might generate spatial vacancies for the accommodation of drug molecules, rendering undetectable signals of SQV in spectrum (II). Spectrum (III) indicated that few spaces existed for the magnetic resonance of the SQV protons in CSLNs with lipid cores of pure CB. This result implied that the resonant ability of the SQV protons was seriously suppressed because of the impediment by crystalline CB. As presented in spectra (II) and (III), the amount of SQV distributed over the exterior layer on CSLNs with lipid cores of pure CB was more than that of a mixture of CA and CB.

3.4. Release of SQV

Fig. 7 shows the profiles of SQV released from CSLNs with lipid cores of pure CB and a mixture of CA and CB. Since CSLNs were continuously shaken in the medium, the superficial structure of the nanoparticles was first deteriorated by the collisions among CSLNs and the fluidic shear forces on particulate surfaces, yielding the release of SQV. For pure CB, a noticeable release of SQV from CSLNs was observed over 6 h, and the release profile became flattened beyond 24 h. This suggested that a number of SQV molecules were excluded by crystalline CB and expelled to the border of lipid cores.

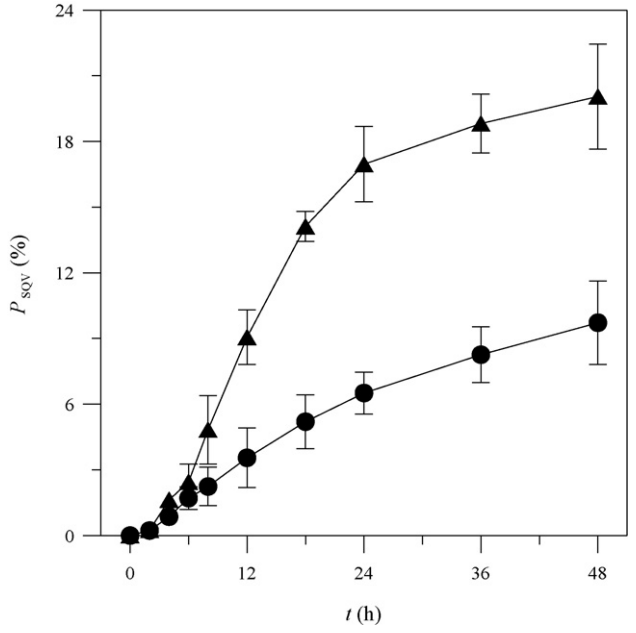

Fig. 7. Temporal variation in the percentage of SQV released from CSLNs. $P_{SA/(DODAB+SA)} = 50\%$, $P_{SQV/(CA+CB+SQV)} = 7.5\%$, $P_{(CA+CB+SQV)/EM} = 4\%$, and $P_{(DODAB+SA)/EM} = 1\%$: (▲) for $P_{CB/(CA+CB)} = 100\%$ and (●) for $P_{CB/(CA+CB)} = 50\%$. $n = 3$.

This result was consistent with the result of ^{1}H NMR in spectrum (III) of Fig. 6. As revealed in Fig. 7, SQV was released gradually from CSLNs with lipid cores of a mixture of CA and CB. If the majority of SQV were located near the particle center, the amount of released SQV in the initial stage would be entirely insignificant. Hence, SQV could most likely be distributed uniformly in lipid cores of the present CSLNs with a mixture of CA and CB. The rate of SQV released from the present CSLNs with lipid cores of a mixture of CA and CB was slower than that of pure CB. This indicated that a lipid core of complicated components would decelerate the delivery of SQV. It could also be concluded that the sustained release of SQV was obtained, and there was nearly no initial burst during the release of entrapped SQV from the present CSLNs.

4. Conclusions

Novel polysorbate 80-stabilized CSLNs composed of nonionic CA and CB in the center of lipid core and cationic SA and DODAB in the periphery of lipid core were prepared in the present study. The results revealed that the entrapment efficiency of SQV in CSLNs was sustained nearly at the same level as the weight percentage of cationic lipid was greater than 1% during emulsification. A mixture of CA and CB was beneficial to the entrapment efficiency. Besides, an increase in the amount of SQV yielded a decrease in the entrapment efficiency. The combinations of SA and DODAB were also advantageous to the entrapment efficiency, and an equal SA and DODAB in CSLNs led to the maximal entrapment efficiencies. Also, a complicated lipid phase could be better for the sustained release of SQV from CSLNs. The present SQV-entrapping CSLNs can be readily applied to the study on the transport behavior across the blood–brain barrier.

Acknowledgment

This work is supported by the National Science Council of the Republic of China.

References

Bachmeier, C.J., Spitzenberger, T.J., Elmquist, W.F., Miller, D.W., 2005. Quantitative assessment of HIV-1 protease inhibitor interactions with drug efflux transporters in the blood–brain barrier. Pharm. Res. 22, 1259–1268.

Bargoni, A., Cavalli, R., Caputo, O., Fundaro, A., Gasco, M.R., Zara, G.P., 1998. Solid lipid nanoparticles in lymph and plasma after duodenal administration to rats. Pharm. Res. 15, 745–750.

Boudad, H., Legrand, P., Lebas, G., Cheron, M., Duchêne, D., Ponchel, G., 2001. Combined hydroxypropyl-β-cyclodextrin and poly(alkylcyanoacrylate) nanoparticles intended for oral administration of saquinavir. Int. J. Pharm. 218, 113–124.

Cross, J., 1987. Nonionic Surfactants: Chemical Analysis. Marcel Dekker, New York, pp. 303–315.

Glynn, S.L., Yazdanian, M., 1998. In vitro blood–brain barrier permeability of nevirapine compared to other HIV antiretroviral agents. J. Pharm. Sci. 87, 306–310.

Jain, R., Duvvuri, S., Kansara, V., Mandava, N.K., Mitra, A.K., 2007. Intestinal absorption of novel-dipeptide prodrugs of saquinavir in rats. Int. J. Pharm. 336, 233–240.

Kim, B.D., Na, K., Choi, H.K., 2005. Preparation and characterization of solid lipid nanoparticles (SLN) made of cacao butter and curdlan. Eur. J. Pharm. Sci. 24, 199–205.

Kuo, Y.C., 2005. Loading efficiency of stavudine on polybutylcyanoacrylate and methylmethacrylate-sulfopropylmethacrylate copolymer nanoparticles. Int. J. Pharm. 290, 161–172.

Kuo, Y.C., Chen, I.C., 2007. Evaluation of surface charge density and surface potential by electrophoretic mobility for solid lipid nanoparticles and human brain-microvascular endothelial cells. J. Phys. Chem. B 111, 11228–11236.

Kuo, Y.C., Chung, C.Y., 2005. Transport of zidovudine- and lamivudine-loaded polybutylcyanoacrylate and methylmethacrylate–sulfopropylmethacrylate nanoparticles across the in vitro blood–brain barrier: characteristics of the drug-delivery system. J. Chin. Inst. Chem. Eng. 36, 627–638.

Kuo, Y.C., Kuo, C.Y., 2008. Electromagnetic interference in the permeability of saquinavir across the blood–brain barrier using nanoparticulate carriers. Int. J. Pharm. 351, 271–281.

Kuo, Y.C., Lin, T.W., 2006. Electrophoretic mobility, zeta potential, and fixed charge density of bovine knee chondrocytes, methylmethacrylate–sulfopropylmethacrylate, polybutylcyanoacrylate, and solid lipid nanoparticles. J. Phys. Chem. B 110, 2202–2208.

Kuo, Y.C., Lin, S.C., 2008. Effect of glutamate on the electrical properties of cationic solid lipid nanoparticles containing stearylamine and dioctadecyldimethyl ammonium bromide. J. Phys. Chem. B 112, 4454–4460.

Kuo, Y.C., Su, F.L., 2007. Transport of stavudine, delavirdine, and saquinavir across the blood–brain barrier by polybutylcyanoacrylate, methylmethacrylate–sulfopropylmethacrylate, and solid lipid nanoparticles. Int. J. Pharm. 340, 143–152.

Lee, V.H., 2000. Membrane transporters. Eur. J. Pharm. Sci. 11, S41–S50.

Lemberg, D.A., Palasanthiran, P., Goode, M., Ziegler, J.B., 2002. Tolerabilities of antiretrovirals in paediatric HIV infection. Drug Safety 25, 973–991.

Liendo, R., Padilla, F.C., Quintana, A., 1997. Characterization of cocoa butter extracted from Criollo cultivars of *Theobroma cacao* L. Food Res. Int. 30, 727–731.

Manjunath, K., Venkateswarlu, V., 2005. Pharmacokinetics, tissue distribution and bioavailability of clozapine solid lipid nanoparticles after intravenous intraduodenal administration. J. Control. Rel. 107, 215–228.

Momot, K.I., Kuchel, P.W., Chapman, B.E., Deo, P., Whittaker, D., 2003. NMR study of the association of propofol with nonionic surfactants. Langmuir 19, 2088–2095.

Müller, R.H., Mäder, K., Gohla, S., 2000. Solid lipid nanoparticles (SLN) for controlled drug delivery—a review of the state of the art. Eur. J. Pharm. Biopharm. 50, 161–177.

Pedersen, N., Hansen, S., Heydenreich, A., Kristensen, H., Poulsen, H., 2006. Solid lipid nanoparticles can effectively bind DNA, streptavidin and biotinylated ligands. Eur. J. Pharm. Biopharm. 62, 155–162.

Polli, J.W., Jarrett, J.L., Studenberg, S.D., Humphreys, J.E., Dennis, S.W., Brouwer, K.R., Woolley, J.L., 1999. Role of P-glycoprotein on the CNS disposition of amprenavir (141W94), an HIV protease inhibitor. Pharm. Res. 16, 1206–1212.

Schubert, M.A., Harms, M., Müller-Goymann, C.C., 2006. Structural investigation on lipid nanoparticles containing high amounts of lecithin. Eur. J. Pharm. Sci. 27, 226–236.

Strazielle, N., Francois, J., Egea, G., 2005. Factors affecting delivery of antiviral drugs to the brain. Rev. Med. Virol. 15, 105–133.

Tabbatt, K., Sameti, M., Olbrich, C., Müller, R.H., Lehr, C.M., 2004. Effect of cationic lipid and matrix lipid composition on solid lipid nanoparticle-mediated gene transfer. Eur. J. Pharm. Biopharm. 57, 155–162.

Wang, J.X., Sun, X., Zhang, Z.R., 2002. Enhanced brain targeting by synthesis of 3′,5′-diocatanoyl-5-fluoro-2′-deoxyuridine and incorporation into solid lipid nanoparticles. Eur. J. Pharm. Biopharm. 54, 285–290.

Westesen, K., Bunjes, H., Koch, M.H.J., 1997. Physicochemical characterization of lipid nanoparticles and evaluation of their drug loading capacity and sustained release potential. J. Control. Rel. 48, 223–236.

Williams, G.C., Sinko, P.J., 1999. Oral absorption of the HIV protease inhibitors: a current update. Adv. Drug Deliv. Rev. 39, 211–238.

Yang, S.C., Lu, L.F., Cai, Y., Zhu, J.B., Liang, B.W., Yang, C.Z., 1999. Body distribution in mice of intravenously injected camptothecin solid lipid nanoparticles and targeting effect of brain. J. Control. Rel. 59, 299–307.